Insulin growth factor signaling is regulated by microRNA-486, an underexpressed microRNA in lung cancer

Yong Peng[a], Yuntao Dai[a], Charles Hitchcock[b], Xiaojuan Yang[c], Edmund S. Kassis[d], Lunxu Liu[e], Zhenghua Luo[a], Hui-Lung Sun[a], Ri Cui[a], Huijun Wei[a], Taewan Kim[a], Tae Jin Lee[a], Young-Jun Jeon[a], Gerard J. Nuovo[b], Stefano Volinia[a], Qianchuan He[f], Jianhua Yu[g], Patrick Nana-Sinkam[h,1], and Carlo M. Croce[a,1]

[a]Department of Molecular Virology, Immunology, and Medical Genetics and [g]Division of Hematology, Comprehensive Cancer Center, The Ohio State University, Columbus, OH 43210; [c]Division of Pharmaceutics, School of Pharmacy and Departments of [b]Pathology and [d]Thoracic Surgery, The Ohio State University, Columbus, OH 43210; [e]Department of Thoracic Surgery, West China Hospital, Sichuan University, Chengdu 610041, China; [f]Public Health Sciences Division, Fred Hutchinson Cancer Research Center, Seattle, WA 98109; and [h]Pulmonary, Allergy, Critical Care, and Sleep Medicine, The Ohio State University Comprehensive Cancer, Columbus, OH 43210

Edited by Webster K. Cavenee, Ludwig Institute for Cancer Research, University of California, San Diego, La Jolla, CA, and approved August 2, 2013 (received for review April 15, 2013)

MicroRNAs (miRNAs) are small 19- to 24-nt noncoding RNAs that have the capacity to regulate fundamental biological processes essential for cancer initiation and progression. In cancer, miRNAs may function as oncogenes or tumor suppressors. Here, we conducted global profiling for miRNAs in a cohort of stage 1 nonsmall cell lung cancers (n = 81) and determined that miR-486 was the most down-regulated miRNA in tumors compared with adjacent uninvolved lung tissues, suggesting that miR-486 loss may be important in lung cancer development. We report that miR-486 directly targets components of insulin growth factor (IGF) signaling including insulin-like growth factor 1 (IGF1), IGF1 receptor (IGF1R), and phosphoinositide-3-kinase, regulatory subunit 1 (alpha) (PIK3R1, or p85a) and functions as a potent tumor suppressor of lung cancer both in vitro and in vivo. Our findings support the role for miR-486 loss in lung cancer and suggest a potential biological link to p53.

Lung cancer is the number one cause of cancer related deaths with a frustratingly poor 5-y survival rate. Despite these statistics, the advent of both early detection and targeted therapies provide support for improved outcomes in the not-too-distant future. Therapies targeted toward specific mutations including Epidermal Growth Factor Receptor (EGFR) and Anaplastic Lymphoid Kinase (ALK) have proven to be of clinical benefit in selected subgroups of patients (1, 2). However, these mutations represent only two of a multitude of mutations in nonsmall cell lung cancer (NSCLC) that could eventually be leveraged for therapeutic purposes. MicroRNAs (miRNAs), a family of short endogenous noncoding RNAs, harbor critical functions in the initiation and progression of a variety of solid and hematological malignancies (3–5). Our laboratory made the early observation that miR-15/16 expression is down-regulated in the majority of cases of chronic lymphocytic leukemia (6). Recently, miRNAs have emerged in NSCLC as both diagnostic and prognostic biomarkers (7, 8). However, the basic mechanisms by which miRNAs function as tumor suppressors or oncogenes in NSCLC and their regulatory factors are known for only a handful of miRNAs.

The Insulin Growth Factor (IGF) pathway is activated in several malignancies including NSCLC (9). In addition, signaling through IGF1R is essential for normal development and growth. Through downstream activation of both PI3K/AKT/mTOR and RAS/RAF/MAP kinase, IGF1R controls cell survival and proliferation respectively (10, 11). Several ongoing clinical trials have focused on strategies for directed targeting of IGF signaling but have had mixed results (12, 13). Despite these results, and given the fundamental role of this axis in tumor initiation and progression, IGF signaling continues to be the focus of investigation particularly for the development of targeted therapeutics in selected subgroups of patients. A few studies to date have validated components of IGF signaling as targets for miRNAs. For example, in breast cancer, miR-148a and miR-152 target both IGF1R and Insulin Receptor Substrate (IRS-1) leading to a reduction in both tumor proliferation and angiogenesis (14). MiR-145 also functions as a potent tumor suppressor in both colon and hepatocellular carcinoma. Components of IGF signaling including IRS-1, IRS-2, and IGF1R have been validated as targets of miR-122 and miR-145 (15–17). Located within the *ankyrin-1* gene (18), miR-486 is deregulated across several solid malignancies (19) including osteosarcoma (20), pancreatic cancer (21), gastric cancer (22), and lung cancer (23). Interestingly, two recent investigations identified miR-486 as a potential noninvasive biomarker for the detection of lung cancer (24–26). To date, investigators have identified a few potential targets for miR-486, including the antiapoptotic OLFM4 (22), SIRT1 (27), and the tumor suppressor PTEN (18). However, the mechanistic role for miR-486 as either an oncogene or tumor suppressor particularly in lung cancer remains largely unknown. In the current study, we conducted a high-throughput miRNA array in a cohort of stage 1 NSCLC (n = 81) and determined that miR-486 was the most decreased miRNA compared with adjacent uninvolved lung tissues. We subsequently demonstrated that miR-486 functions as a potent suppressor of cellular proliferation, migratory capacity, and tumor growth both in vitro and in vivo. Furthermore, we validated components of IGF signaling including IGF1, IGF1R, and p85α as targets of miR-486. Lastly, we determined that the biological effects of miR-486 are partially dependent upon intact p53.

Results

miR-486 Is Down-Regulated in NSCLC. We conducted a high throughput miRNA array on a cohort of stage 1 adenocarcinomas (n = 81). Among the deregulated miRNAs, we identified several miRNAs that have been previously implicated in lung cancer including miR-21 (up-regulated) and miR-126 (down-regulated). However, miR-486 was the most down-regulated miRNA in lung tumors compared with adjacent uninvolved lung tissues (fold

Author contributions: Y.P. and C.M.C. designed research; Y.P., Y.D., C.H., X.Y., E.S.K., Z.L., H.-L.S., R.C., H.W., T.K., T.J.L., Y.-J.J., and G.J.N. performed research; L.L. contributed new reagents/analytic tools; Y.P., S.V., Q.H., J.Y., P.N.-S., and C.M.C. analyzed data; and Y.P., J.Y., P.N.-S., and C.M.C. wrote the paper.

The authors declare no conflict of interest.

This article is a PNAS Direct Submission.

[1]To whom correspondence may be addressed. E-mail: carlo.croce@osumc.edu or Patrick.nana-Sinkam@osumc.edu.

This article contains supporting information online at www.pnas.org/lookup/suppl/doi:10.1073/pnas.1307107110/-/DCSupplemental.

A

Altered expressed microRNAs in NSCLC tumors

mature miR	p value	FDR,%	fold change
hsa-miR-486	<1e-07	<1e-07	0.12
hsa-miR-126*	<1e-07	<1e-07	0.30
hsa-miR-30c	<1e-07	<1e-07	0.33
hsa-miR-325	<1e-07	<1e-07	0.34
hsa-miR-140-3p	<1e-07	<1e-07	0.34
hsa-miR-30d	<1e-07	<1e-07	0.35
hsa-miR-30a	<1e-07	<1e-07	0.37
hsa-miR-451	1.00e-07	1.45e-06	0.42
hsa-miR-184	<1e-07	<1e-07	0.43
hsa-miR-126	2.00e-07	2.62e-06	0.43
hsa-miR-625*	0.004414	0.00278	1.54
hsa-miR-532-5p	0.014069	0.00716	1.56
hsa-miR-25*	0.0004857	0.00278	1.56
hsa-miR-663	0.000626	0.00351	1.58
hsa-miR-375	0.0077897	0.0298	1.61
hsa-miR-551a	1.40e-06	1.37e-05	1.71
hsa-miR-187	0.0004495	0.0267	1.84
hsa-miR-650	3.3e-06	3.13e-05	2.42
hsa-miR-21	<1e-07	<1e-07	3.8

FDR: false discovery rate

B

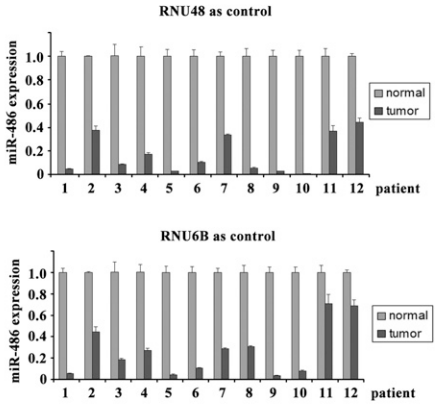

Fig. 1. Down-regulation of miR-486 expression in NSCLC patients. Total RNAs were isolated from cancerous and adjacent normal tissues of formalin-fixed, paraffin-embedded samples, and then subjected to miRNA microarray. (*A*) The most down-regulated and up-regulated miRNAs. (*B*) Down-regulation of miR-486 was validated in 12 patient samples by real-time PCRs using either RNU48 or RNU6B as control.

change: 0.12) (Fig. 1*A*). We subsequently validated this finding by quantitative RT-PCR (qRT-PCR) for both miR-486 and another deregulated miRNA (miR-140-3p) in an independent group of 12 paired NSCLC and adjacent tissues (Fig. 1*B* and Fig. S1).

miR-486 Reduces Growth and Migration in NSCLC in Vitro. Given the low expression of miR-486 in lung tumors, we hypothesized that miR-486 may function as a tumor suppressor. We transiently transfected miR-486 in two independent NSCLC cell lines, A549 and H460, and demonstrated that miR-486 overexpression led to a reduction in cellular proliferation in both cell lines (Fig. 2*A*). In addition, H460 and A549 harboring miR-486 gain of function showed lower colony formation (Fig. 2*B*). We next examined the effects of miR-486 on cell-cycle progression in H460 cells and observed a significant increase in sub-G0 and G1 phase, suggesting increased cell-cycle arrest and apoptosis (Fig. 2*C*). Lastly, miR-486 reduced migratory capacity in A549 cells (Fig. 2*D*).

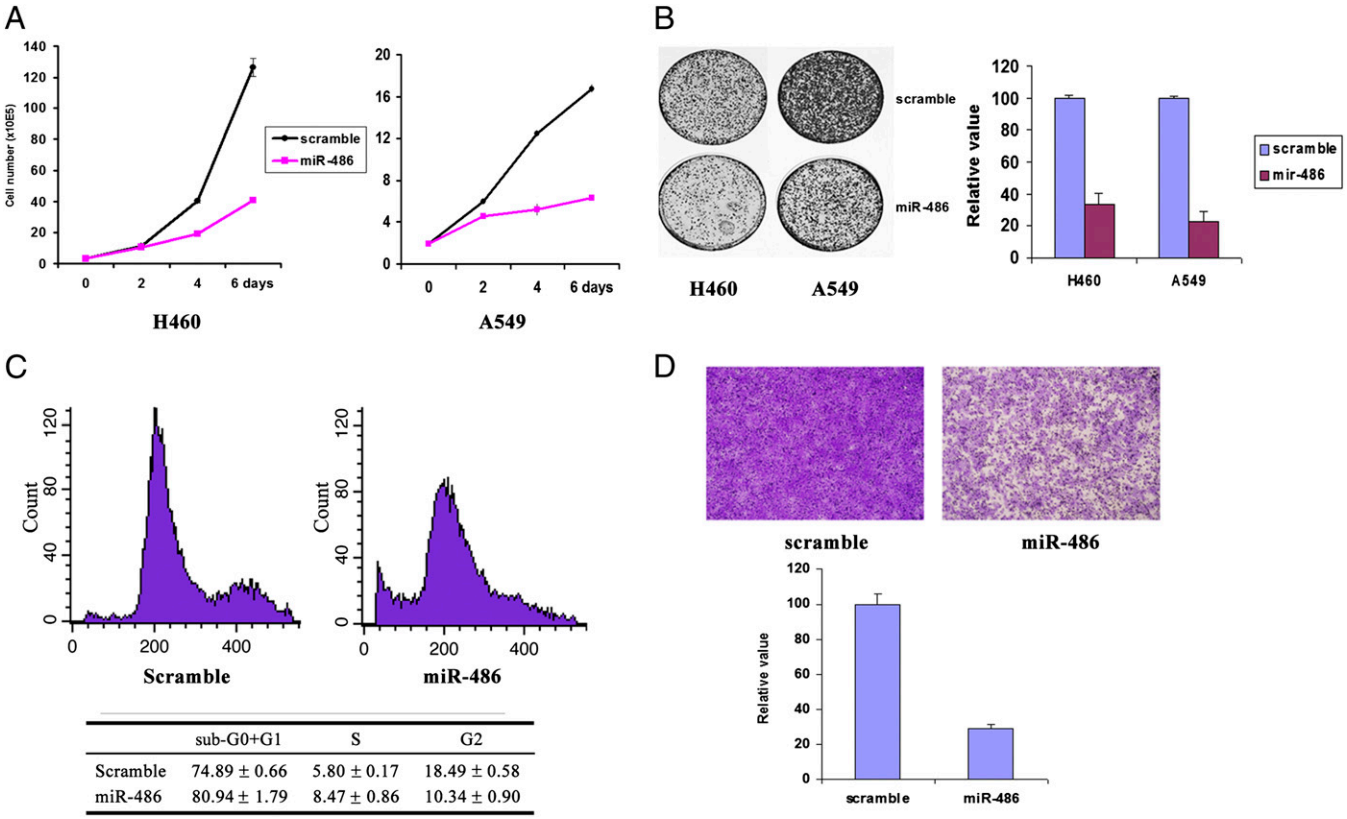

	sub-G0+G1	S	G2
Scramble	74.89 ± 0.66	5.80 ± 0.17	18.49 ± 0.58
miR-486	80.94 ± 1.79	8.47 ± 0.86	10.34 ± 0.90

Fig. 2. Ectopic expression of miR-486 affects cell growth, colony formation, cell cycle, and cell migration. (*A* and *B*) miR-486 overexpression inhibits cell growth and colony formation. (*A*) H460 or A549 cells were transfected with scramble or premiR-486, and viable cells were counted with trypan blue to measure cell growth. (*B*) Cell colonies were stained with crystal violet solution, dissolved in Sorenson's buffer and then measure OD590nm for quantification. (*C*) Flow cytometric distribution of H460 cells transfected with scramble or premiR-486. (*D*) miR-486 decreases cell migration. A549 cells transfected with scramble or premiR-486 were seeded in Transwell plate and incubated at 37 °C for 24 h. The migrated cells were stained with crystal violet solution, dissolved in Sorenson's buffer, and then measured at OD590nm for quantification. Data are presented as ±SD.

miR-486 Targets the 3′UTR for p85α, IGF1R, and IGF1. Using in silico prediction programs, we identified several components of the IGF tyrosine kinase signaling pathway as potential targets for miR-486. In particular, the 3′ untranslated regions (UTR) of p85α, IGF1R, and IGF1 mRNA harbored sequences complementary to the miR-486 seed sequence (Fig. 3*A* and Fig. S2*A*). To verify whether p85α, IGF1R, and IGF1 are direct targets of miR-486, we cloned each 3′ UTR into the psiCHECK2 vector downstream of luciferase ORF. In addition, to validate target specificity, we conducted site-directed mutagenesis for each 3′ UTR using the QuikChange Mutagenesis kit to destroy the miR-486 binding sites. When we cotransfected A549 cells with each of the three cloned UTRs and miR-486, we observed a consistent reduction in luciferase activity for all 3′ UTRs by miR-486 (Fig. 3*B* and Fig. S2*B*). Conversely, cotransfection of miR-486 with the mutated forms of the 3′ UTRs resulted in no significant change in luciferase activity (Fig. 3*B* and Fig. S2*B*), suggesting miRNA/target 3′ UTR specificity. We next examined for the effects of miR-486 overexpression on target mRNA and protein expression in two independent cell lines. Interestingly, miR-486 reduced both mRNA and protein expression for p85α in A549 and H460 cells (Fig. 3 *C* and *D*), whereas it reduced only protein expression for IGF1R in both cell lines (Fig. 3 *C* and *D*). In addition, we validated IGF1 as target for miR-486 (Fig. S2 *B* and *C*). IGF signaling has been extensively investigated in lung cancer. Given that we validated components of this pathway as targets of miR-486, we sought to examine downstream signaling. We demonstrated in both H1299 and H460 cell lines that miR-486 overexpression resulted in decreased p110α, pAKT (Ser473), and pFoxo3a protein expression (Fig. 3*E*). Given the reduction in pAKT and pFoxo3a, we observed a resultant increase in the cyclin-dependent kinase inhibitor p27. In addition, we examined expression of these target proteins by Western blot and tissue microarray in an independent cohort of lung cancer patients. We demonstrated that p85α, IGF1R, and IGF1 were overexpressed, whereas miR-486 expression was decreased in most of the cancerous tissues of NSCLC patients (Fig. S3).

Selective Targeting of p85α and IGF1R Induces Cell Cycle Arrest and Reduces Migration in NSCLC. To determine whether the biological effects of miR-486 were indeed attributable to direct targeting of components of IGF signaling, we conducted siRNA based silencing of both p85α and IGF1R and assessed cells for both cell cycle progression and migratory capacity. We observed that siRNA mediated knockdown of p85α resulted in a significant increase in cells in G1 phase, whereas IGF1R knockdown lead to a slight increase in cells in sub-G0 phase (Fig. 4 *B* and *C*). Interestingly, combining knockdown of both targets resulted in no additional change in sub-G0 and G1 phase cell numbers. We next showed that knockdown of p85α and IGF1R, both alone and in combination, decreased migratory capacity of cancer cells (Fig. 4 *D* and *E*). Our results suggest that the observed effects of miR-486 on cell cycle progression and cell migration are partially mediated through miR-486 targeting of p85α and IGF1R.

p53 Regulates miR-486 Expression. The tumor suppressor p53 is the most frequently altered gene in human cancers. In our preliminary studies, we observed a trend toward p53 wild-type cell lines having higher miR-486 expression than other non-wild-type cell lines with some exceptions (Fig. S4). Thus, we sought to investigate whether p53 expression was involved in miR-486 induction. Nutilin-3 is a small molecule inhibitor of the p53/MDM2 that leads to p53 stabilization and activation. We treated two p53 wild-type lung cancer cell lines (H460 and A549) and one p53-null cell line (H1299) with Nutilin-3 (10 μM) for 24 h and assessed miR-486 expression by qRT-PCR. Nutilin-3 treatment

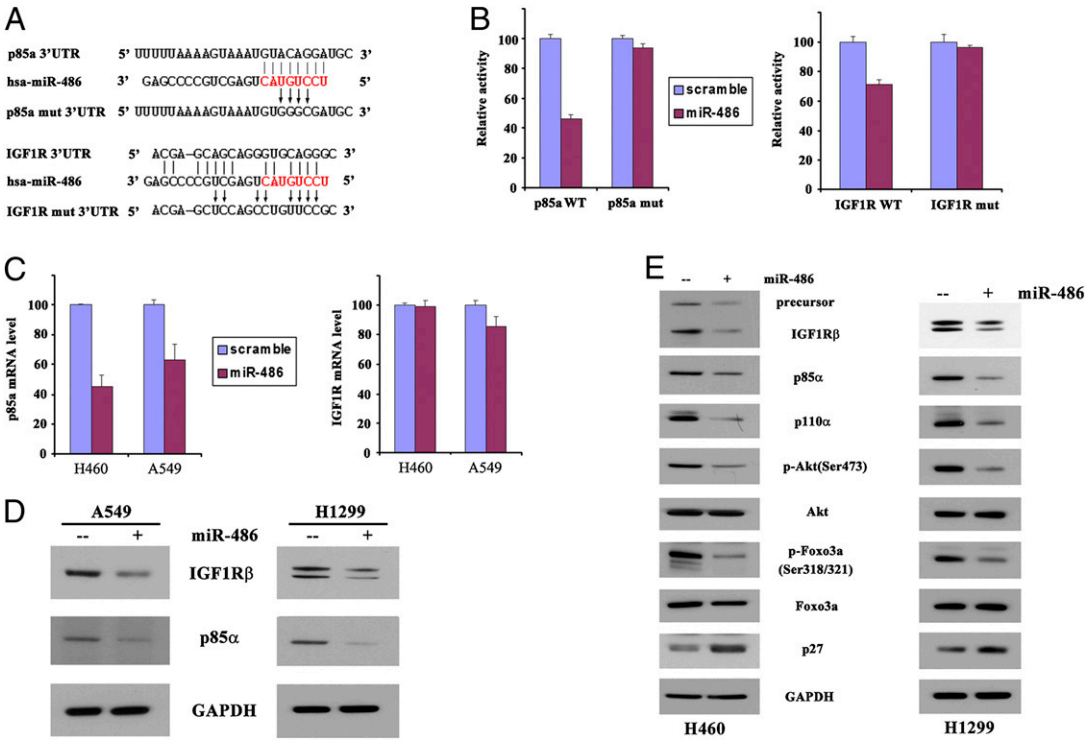

Fig. 3. p85α and IGF1R are direct targets of miR-486. (*A*) p85α and IGF1R 3′UTRs contain predicted miR-486 binding sites. The figures show alignment of miR-486 with p85α and IGF1R 3′UTRs and the arrows indicate the mutagenesis nucleotides. (*B*) Dual luciferase reporter assay. Luciferase reporter constructs containing wild-type or mutated p85α and IGF1R 3′ UTRs were cotransfected with scramble or premiR-486 into A549 cells. Relative firefly luciferase expression was normalized to Renilla luciferase. (*C* and *D*) qRT-PCR and Western blot to measure p85α and IGF1R mRNA and protein level in cells transfected with scramble or premiR-486 for 72 h. (*E*) Effect of miR-486 on Akt/Foxo3a pathway. H1299 or H460 cells were transfected with scramble or premiR-486 for 72 h, total proteins were prepared for Western blot.

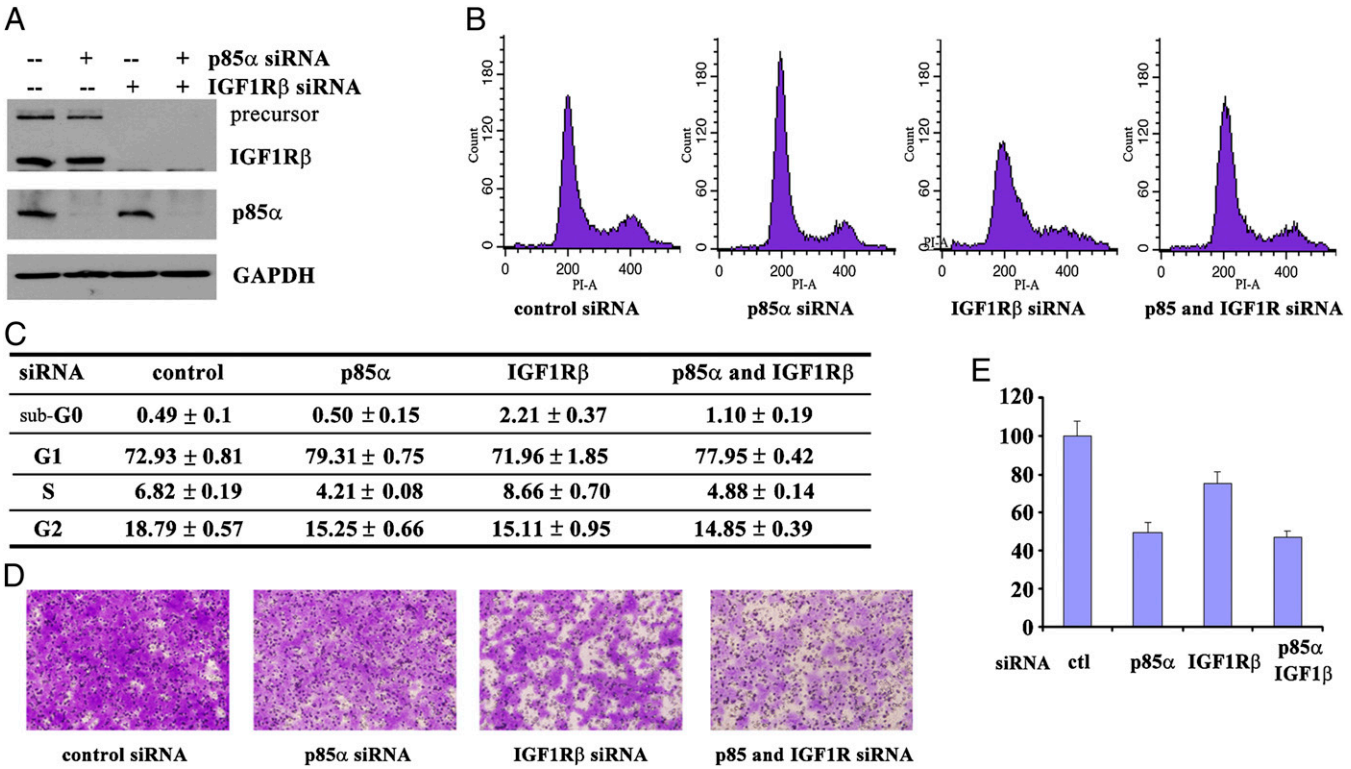

Fig. 4. Effect of p85α and IGF1R knockdown on cell cycle and cell migration. (*A*) Western blot of H460 cells transfected with scramble, p85 siRNA, IGF1R siRNA, or both siRNAs for 48 h. (*B*) Flow cytometry of H460 cells transfected with scramble, p85 siRNA, IGF1R siRNA, or both siRNAs for 48 h. The quantification data are shown in *C*. (*D*) Cell migration of A549 cells transfected with siRNAs against p85a and IGF1R alone and in combination in Transwell plates at 37 °C for 24 h. The migrated cells were stained with crystal violet solution, dissolved in Sorenson's buffer, and then measured at OD590nm for quantification (*E*).

resulted in a significant induction of miR-486 expression in both p53 wild-type cell lines but not in the mutant p53 cell line (Fig. 5*A*). To determine whether Nutlin-3–induced miR-486 expression is p53 dependent, siRNA was used to efficiently knock down p53 expression in both A549 and H460 cells (Fig. S5). p53 knockdown attenuated the induction of miR-486 expression by Nutlin-3 treatment (Fig. 5*B*). This was also supported by the observation that transfection of p53 into a p53-null cell line (H1299) resulted in increased miR-486 expression (Fig. S6). We also observed higher miR-486–expression levels in HCT116 ($p53^{+/+}$) cells compared with HCT116 ($p53^{-/-}$) cells (Fig. S7). We also mapped a p53 binding site to a DNA region upstream of the miR-486 gene (Fig. 5*C*). The predicted p53 binding sequence was then identified by Chromatin Immunoprecipitation (ChIP) using anti-p53 antibody. The p21 promoter was used as a positive control. In the no-treatment setting, there was no evidence of p53 binding to miR-486 promoter (Fig. 5*D*, *Left*). However, upon p53 activation by Nutilin-3 treatment, we observed significant p53 binding to both regions of miR-486 (Fig. 5*D*, *Right*). In both cases, negative controls using IgG failed to reveal any binding. We subsequently cloned the genomic sequence containing this p53 binding site into pGL4.27 luciferase vector and assessed luciferase activity. Overexpression of p53 caused a significant induction of luciferase activity, and both single and double mutations at p53 binding sites attenuated this effect (Fig. 5*E*), suggesting such sites are indeed p53 binding sites.

miR-486 Induction of Apoptosis Is Dependent on p53. Previous studies have suggested that miR-486 targets cancer cell survival in other solid malignancies (22, 28). As a result, we sought to determine whether similar effects were present in lung cancer. Overexpression of miR-486 induced apoptosis as measured by caspase 3/7 activity in both p53 wild-type cell lines (H460 and A549) but not in a p53 mutant line (H1299) (Fig. 5*G*, *Left*). To determine whether these differences were indeed p53 dependent, we conducted a similar experiment in the setting of selective siRNA mediated p53 knockdown. p53 knockdown decreased the induction in apoptosis mediated by miR-486 overexpression suggesting that p53 activity is necessary for the effects of miR-486 on apoptosis (Fig. 5*G*, *Right*). These findings were further validated by Western blot analysis (Fig. 5*H*), which shows induction in apoptotic proteins including cleaved caspase 3, 7, and poly (ADP-ribose) polymerase 1 (PARP1) in miR-486 overexpressing A549 cells but not H1299 cells. Moreover, forced expression of miR-486 resulted in increased expression of p53 upregulated modulator of apoptosis (PUMA) (Fig. S8), a proapoptotic p53 target, and this induction was attenuated by p53 knockdown (Fig. 5*F*), supporting our finding that p53 is involved in miR-486–induced apoptosis.

Effects of miR-486 on Tumorigenicity in Vivo. miR-486 is deregulated in several solid malignancies, including lung cancer. In addition, miR-486 has been identified as both a diagnostic and prognostic biomarker in lung cancer (24–26). To determine the role for miR-486 in vivo, both A549 and H1299 cell lines with or without overexpressing miR-486 were injected s.c. into the flanks of nude mice. Within 24 d after injection, overexpression of miR-486 in both H1299 cells caused a substantial reduction in tumor volume in vivo (Fig. 6 *A*–*C*). Moreover, Western blot analysis showed that expression of IGF1R and p85α is reduced in miR-486 overexpressing tumors (Fig. 6*D*). A549 cells overexpressing miR-486 did not form any detectable xenograft tumors, whereas control cells formed tumors. These in vivo data demonstrate that miR-486 functions as a tumor suppressor.

Discussion

IGF signaling has been implicated in the pathogenesis of a variety of diseases including lung cancer and as a result has been the

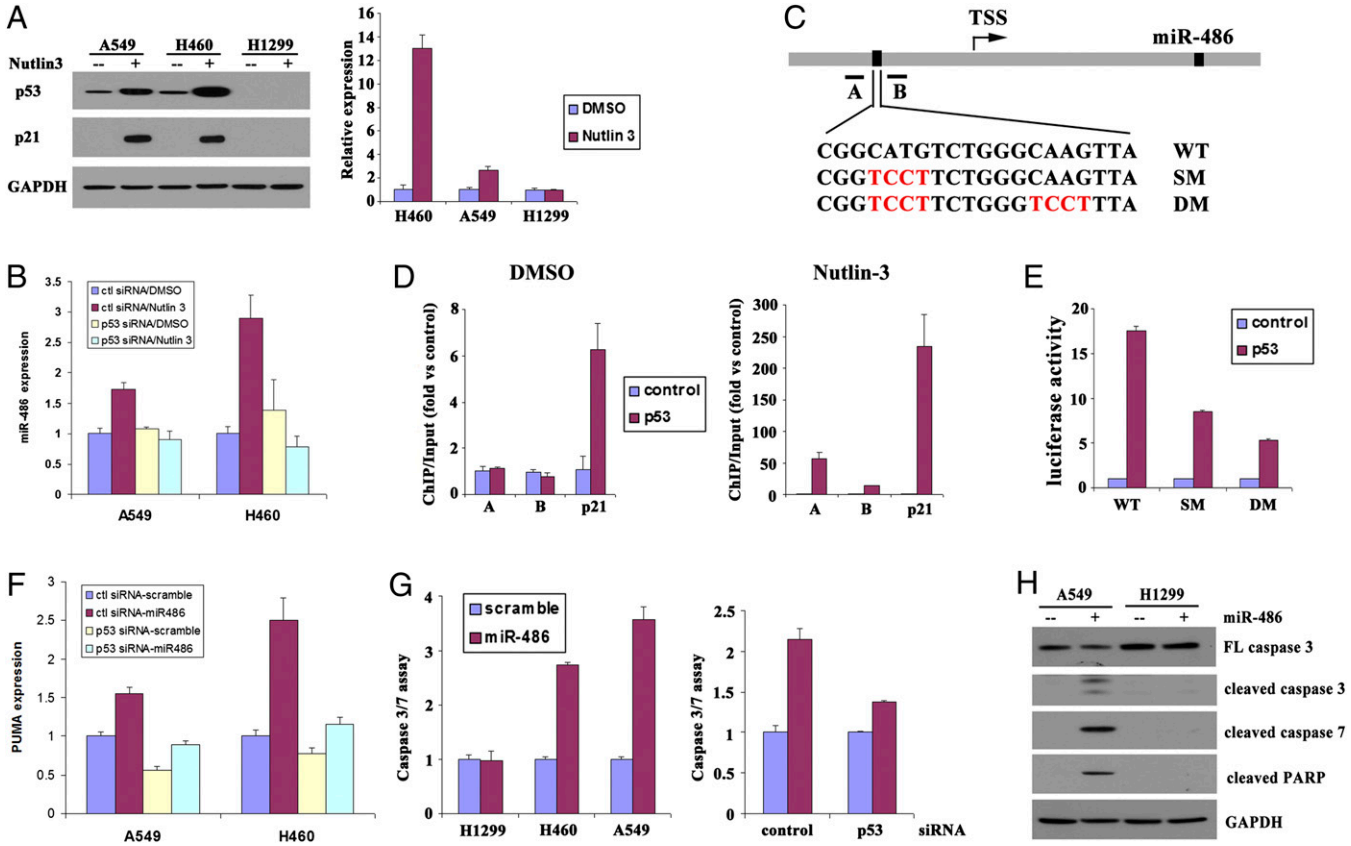

Fig. 5. p53-regulated miR-486 activates p53 pathway. (*A*) Western blot and qRT-PCR of miR-486 expression in cells treated with vehicle DMSO or 10 μM Nutlin-3 for 24 h. RNU48 was used for normalization. (*B*) qRT-PCR of miR-486 expression in cells first transfected with control or p53 siRNA, followed by treatment with DMSO or 10 μM Nutlin-3 for 24 h. (*C*) The diagram indicates predicted p53 binding sites and its single (SM) or double mutants (DM). The bars show PCR amplicon for ChIP assay. (*D*) p53 association of miR-486 promoter after Nutlin-3 treatment. A549 cells were treated with DMSO (*Left*) or 10 μM Nutlin-3 (*Right*) for 24 h, and then subjected to ChIP assays. p53 binding site of p21 promoter was used for positive control. (*E*) Dual luciferase assay. A549 cells were transfected with reporter constructs containing wild type (WT), single mutation (SM), or double mutation (DM) of p53 binding sites plus empty vector or p53-expressing plasmid. Firefly luciferase activities were normalized by Renilla luciferase activities, and then normalized to empty vector. (*F*) miR-486 induces PUMA expression through p53. A549 and H460 cells were transfected with control or p53 siRNA for 24 h, followed by transfection with scramble or miR-486 for 32 h. Total RNAs were subjected to qRT-PCR to measure PUMA mRNA levels. (*G*) miR-486 induces apoptosis in A549 and H460 cells. (*Left*) Caspase 3/7 activity assays were performed in cells transfected with scramble or premiR-486. (*Right*) Knockdown of p53 in H460 cells inhibits miR-486–induced caspase 3/7 assay. (*H*) Western blot analysis of proteins from A549 or H1299 cells transfected with scramble or premiR-486 for 48 h.

focus of targeted therapeutics (29, 30). In particular, signaling through IGF1 and IGF2 and subsequent downstream mediators can regulate fundamental processes including cellular proliferation, differentiation and migration (31). Previous studies demonstrate that components of IGF signaling including IGF1R are overexpressed in NSCLC and that deregulation of IGF signaling may contribute to resistance to other tyrosine kinase receptor inhibitors such as EGFR inhibitors (32). These findings have served as the primary impetus for clinical trials combining IGF signaling and EGFR inhibition as targeted therapies. MiRNAs can functionally target IGF signaling in hepatocellular, colon and breast carcinoma (15–17). However, the link between miRNAs and IGF signaling in lung cancer is relatively unknown. We conducted a miRNA array on lung tumors from 81 patients with stage 1 adenocarcinoma and identified miR-486 to be the most decreased miRNA. Localized to the *ankyrin-1* gene, miR-486 may function as cell-specific tumor suppressor or oncogene. In lung cancer, miR-486 has emerged as a noninvasive biomarker with detection in both the plasma and sputum (24, 26). Here we demonstrated that miR-486 functions as a potent tumor suppressor in lung cancer reducing both proliferative and migratory capacity as well as inducing apoptosis in lung cancer cell lines. We have validated several components of IGF signaling, including IGF1R, p85α, and IGF1 as direct targets of miR-486 resulting in a reduction in downstream pAKT and pFoxo3a. Conversely, Small and colleagues recently demonstrated that miR-486 targeted both PTEN and Foxo1a leading to an actual increase in PI3K/AKT signaling, thus further supporting the cell-specific effects of miR-486 (18). To determine whether the observed biological effects of miR-486 were in fact mediated through our validated targets, we examined the effects of selective knockdown of both p85α and IGF1R on both cell cycle progression and migration. Although p85α had a more robust effect on cell cycle, both targets reduced migratory capacity of lung cancer cells. Our current understanding regarding the regulatory mechanisms of miR-486 is based on studies focused on muscle pathology. Glucose, serum response factor, and myocardin-related transcription factor are all regulators of miR-486 (18, 27). Given our observations that p53 wild-type and null cell lines had differential expression of miR-486, we sought to determine whether there was a link between miR-486 levels and p53 status. We validated a functional p53 binding site in miR-486. We also assessed whether the miR-486–induced effects on apoptosis were mediated through p53. We observed that selective silencing of p53 abrogated the effects of miR-486 on apoptosis in lung cancer cell lines, suggesting such a relationship. Lastly, we assessed the effects of miR-486 on in vivo tumorigenicity using a xenograft nude mouse model. Mice harboring miR-

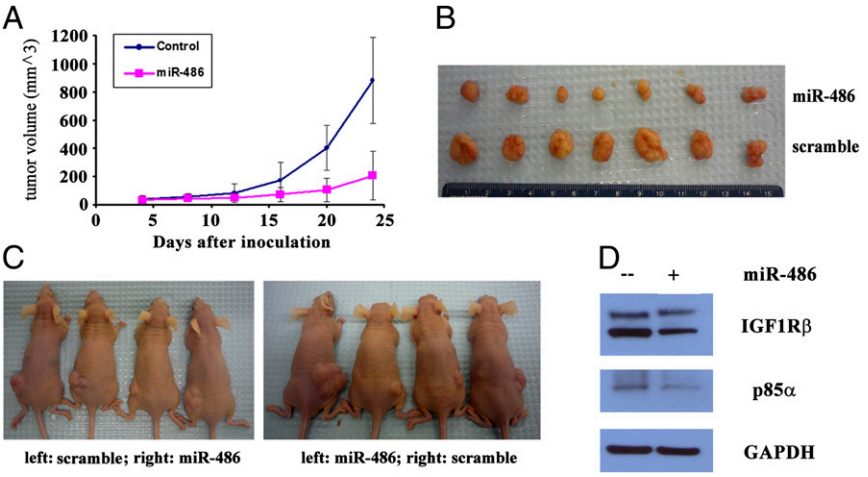

Fig. 6. miR-486 inhibits tumor growth in xenograft model. (*A*) Tumor growth in nude mice s.c. injected into the flanks with H1299 cells transfected with scramble or premiR-486. Data are represented as mean ± SD ($n = 8$ per group). (*B* and *C*) Comparison of tumor engraftment sizes in nude mice injected with H1299 cells transfected with scramble or pre-miR-486. (*D*) Western blot analysis of protein lysates from xenograft tumors.

486–overexpressing cell lines had a significant reduction in xenograft tumor size compared with control animals. In summary, we have identified a biological mechanism for miR-486 as a tumor suppressor in lung cancer through targeting of components of IGF signaling (Fig. 6*D*). In addition, we have identified a potential link between miR-486 and p53 status suggesting that miR-486 effect on apoptosis is partially dependent upon intact p53. This raises the potential for miR-486 to serve as a biomarker in future IGF-based targeted studies.

Materials and Methods

NSCLC Samples and miRNA Microarray. Protein lysates from eight NSCLC patients were obtained from P.N.-S. Human NSCLC tissue arrays LC10012 were purchased from US Biomax. In total, 81 cases of stage I of human NSCLC samples were histologically confirmed by C.H. according to H&E staining, and formalin-fixed, paraffin-embedded tissues were sent to The Ohio State University Pathology Core Facility to microdissect out cancerous tissues and its adjacent normal tissues for total RNA isolation by RecoverALL Total Nucleic Acid Isolation kit (Ambion). Tissues were obtained under an Ohio State University approved Institutional Review Board protocol, and written informed consent was obtained from patients before sample analyses. Five micrograms of total RNA was reverse-transcribed with biotin end-labeled random oligonucleotide primers, and cDNA was hybridized to miRNA microarray chips (OSU-CCC version 4.0). Biotin-containing transcripts were detected with streptavidin-Alexa647 conjugate and scanned and analyzed by using an Axon 4000B scanner and GenePix 6.0 software (Axon Instruments). The mean fluorescence intensity of replicate spots was substracted from background and normalized by using global median method.

A detailed description of the materials and methods used in this study are found in *SI Materials and Methods*. For additional details on plasmid construction, target analysis, cell culture and transfection, Western blot analysis, animal study, and statistical analysis, please see *SI Materials and Methods*.

ACKNOWLEDGMENTS. We thank Prof. Bert Vogelstein (Johns Hopkins University) for the HCT-116 cells. This work was supported by National Institutes of Health Grant U01 CA152758 (to C.M.C.).

1. Rosell R, et al. (2012) Erlotinib versus standard chemotherapy as first-line treatment for European patients with advanced EGFR mutation-positive non-small-cell cancer. *Lancet Oncol* 13(3):239–246.
2. Gandhi L, Jänne PA (2012) Crizotinib for ALK-rearranged non-small cell lung cancer: A new targeted therapy for a new target. *Clin Cancer Res* 18(14):3737–3742.
3. Calin GA, et al. (2004) Human microRNA genes are frequently located at fragile sites and genomic regions involved in cancers. *Proc Natl Acad Sci USA* 101(9):2999–3004.
4. Croce CM (2009) Causes and consequences of microRNA dysregulation in cancer. *Nat Rev Genet* 10(10):704–714.
5. Nana-Sinkam SP, Croce CM (2013) Clinical applications for microRNAs in cancer. *Clin Pharmacol Ther* 93(1):98–104.
6. Cimmino A, et al. (2005) miR-15 and miR-16 induce apoptosis by targeting BCL2. *Proc Natl Acad Sci USA* 102(39):13944–13949.
7. Boeri M, et al. (2011) MicroRNA signatures in tissues and plasma predict development and prognosis of computed tomography detected lung cancer. *Proc Natl Acad Sci USA* 108(9):3713–3718.
8. Shen J, Jiang F (2012) Application of microRNAs in diagnosis and prognosis in lung cancer. *Expert Opin Med Diagn* 6(3):197–207.
9. Scagliotti GV, Novello S (2012) The role of the insulin-like growth factor signaling pathway in non-small cell lung cancer and other solid tumors. *Cancer Treat Rev* 38(4): 292–302.
10. LeRoith D, Helman L (2004) The new kid on the block(ade) of the IGF-1 receptor. *Cancer Cell* 5(3):201–202.
11. Pollak M (2012) The insulin and insulin-like growth factor receptor family in neoplasia: An update. *Nat Rev Cancer* 12(3):159–169.
12. Karp DD, et al. (2009) Safety, pharmacokinetics, and pharmacodynamics of the insulin-like growth factor type 1 receptor inhibitor figitumumab (CP-751,871) in combination with paclitaxel and carboplatin. *J Thorac Oncol* 4(11):1397–1403.
13. Ramalingam SS, et al. (2011) Randomized phase II study of erlotinib in combination with placebo or R1507, a monoclonal antibody to insulin-like growth factor-1 receptor, for advanced-stage non-small-cell lung cancer. *J Clin Oncol* 29(34):4574–4580.
14. Xu Q, et al. (2013) A regulatory circuit of miR-148a/152 and DNMT1 in modulating cell transformation and tumor angiogenesis through IGF-IR and IRS1. *J Mol Cell Biol* 5(1):3–13.
15. Shi B, et al. (2007) Micro RNA 145 targets the insulin receptor substrate-1 and inhibits the growth of colon cancer cells. *J Biol Chem* 282(45):32582–32590.
16. Law PT, et al. (2012) MiR-145 modulates multiple components of the insulin-like growth factor pathway in hepatocellular carcinoma. *Carcinogenesis* 33(6):1134–1141.
17. Wang B, Wang H, Yang Z (2012) MiR-122 inhibits cell proliferation and tumorigenesis of breast cancer by targeting IGF1R. *PLoS ONE* 7(10):e47053.
18. Small EM, et al. (2010) Regulation of PI3-kinase/Akt signaling by muscle-enriched microRNA-486. *Proc Natl Acad Sci USA* 107(9):4218–4223.
19. Navon R, et al. (2009) Novel rank-based statistical methods reveal microRNAs with differential expression in multiple cancer types. *PLoS ONE* 4(11):e8003.
20. Namløs HM, et al. (2012) Modulation of the osteosarcoma expression phenotype by microRNAs. *PLoS ONE* 7(10):e48086.
21. Ali S, Saleh H, Sethi S, Sarkar FH, Philip PA (2012) MicroRNA profiling of diagnostic needle aspirates from patients with pancreatic cancer. *Br J Cancer* 107(8):1354–1360.
22. Oh HK, et al. (2011) Genomic loss of miR-486 regulates tumor progression and the OLFM4 antiapoptotic factor in gastric cancer. *Clin Cancer Res* 17(9):2657–2667.
23. Tan X, et al. (2011) A 5-microRNA signature for lung squamous cell carcinoma diagnosis and hsa-miR-31 for prognosis. *Clin Cancer Res* 17(21):6802–6811.
24. Yu L, et al. (2010) Early detection of lung adenocarcinoma in sputum by a panel of microRNA markers. *Int J Cancer* 127(12):2870–2878.
25. Shen J, et al. (2011) Diagnosis of lung cancer in individuals with solitary pulmonary nodules by plasma microRNA biomarkers. *BMC Cancer* 11:374.
26. Hu Z, et al. (2010) Serum microRNA signatures identified in a genome-wide serum microRNA expression profiling predict survival of non-small-cell lung cancer. *J Clin Oncol* 28(10):1721–1726.
27. Kim YJ, et al. (2012) miR-486-5p induces replicative senescence of human adipose tissue-derived mesenchymal stem cells and its expression is controlled by high glucose. *Stem Cells Dev* 21(10):1749–1760.
28. Narducci MG, et al. (2011) MicroRNA profiling reveals that miR-21, miR486 and miR-214 are upregulated and involved in cell survival in Sézary syndrome. *Cell Death Dis* 2:e151.
29. Neal JW, Sequist LV (2010) Exciting new targets in lung cancer therapy: ALK, IGF-1R, HDAC, and Hh. *Curr Treat Options Oncol* 11(1-2):36–44.
30. Tognon CE, Sorensen PH (2012) Targeting the insulin-like growth factor 1 receptor (IGF1R) signaling pathway for cancer therapy. *Expert Opin Ther Targets* 16(1):33–48.
31. Yu H, Rohan T (2000) Role of the insulin-like growth factor family in cancer development and progression. *J Natl Cancer Inst* 92(18):1472–1489.
32. Dziadziuszko R, et al. (2010) Insulin-like factor receptor1 (IGF1R) gene copy number is associated with survival in operable non-small-cell lung cancer. *J Clin Oncol* 28(13): 2174–2180.